

1 **Meta-analysis of fecal metagenomes reveals global microbial signatures that** 2 **are specific for colorectal cancer**

4 **Authors**

5 Jakob Wirbel^{1*}, Paul Theodor Pyl^{2,3*}, Ece Kartal^{1,4}, Konrad Zych¹, Alireza Kashani², Alessio Milanese¹,
6 Jonas S Fleck¹, Anita Y Voigt^{1,5}, Albert Palleja², Ruby P Ponnudurai¹, Shinichi Sunagawa^{1,6}, Luis
7 Pedro Coelho^{1,‡}, Petra Schrotz-King⁷, Emily Vogtmann⁸, Nina Habermann⁹, Emma Niméus^{3,10}, Andrew
8 M Thomas^{11,12}, Paolo Manghi¹¹, Sara Gandini¹³, Davide Serrano¹³, Sayaka Mizutani^{14,15}, Hirotsugu
9 Shiroma¹⁴, Satoshi Shiba¹⁶, Tatsuhiro Shibata^{16,17}, Shinichi Yachida^{16,18}, Takuji Yamada^{14,19}, Levi
10 Waldron^{20,21}, Alessio Naccarati^{22,23}, Nicola Segata¹¹, Rashmi Sinha⁸, Cornelia M. Ulrich²⁴, Hermann
11 Brenner^{7,25,26}, Manimozhayan Arumugam^{2,27+}, Peer Bork^{1,4,28,29+}, Georg Zeller¹⁺

13 **Affiliations**

- 14 1. Structural and Computational Biology Unit, European Molecular Biology Laboratory (EMBL),
15 Heidelberg, Germany
- 16 2. Novo Nordisk Foundation Center for Basic Metabolic Research, Faculty of Health and
17 Medicine, University of Copenhagen, Copenhagen, Denmark
- 18 3. Division of Surgery, Oncology and Pathology, Department of Clinical Sciences Lund, Faculty
19 of Medicine, Lund University, Sweden
- 20 4. Molecular Medicine Partnership Unit (MMPU), Heidelberg, Germany
- 21 5. The Jackson Laboratory for Genomic Medicine, Farmington, Connecticut, USA
- 22 6. Department of Biology, ETH Zürich, Zürich, Switzerland
- 23 7. Division of Preventive Oncology, National Center for Tumor Diseases (NCT) and German
24 Cancer Research Center (DKFZ), Heidelberg, Germany
- 25 8. Division of Cancer Epidemiology and Genetics, National Cancer Institute, Bethesda,
26 Maryland, USA
- 27 9. Genome Biology Unit, European Molecular Biology Laboratory (EMBL), Heidelberg, Germany
- 28 10. Division of Surgery, Department of Clinical Sciences Lund, Faculty of Medicine, Skane
29 University Hospital, Lund, Sweden
- 30 11. Department CIBIO, University of Trento, Trento, Italy.
- 31 12. Biochemistry Department, Chemistry Institute, University of São Paulo, São Paulo, Brazil.
- 32 13. IEO, European Institute of Oncology IRCCS, Milan, Italy.
- 33 14. School of Life Science and Technology, Tokyo Institute of Technology, Tokyo, Japan
- 34 15. Research Fellow of Japan Society for the Promotion of Science
- 35 16. Division of Cancer Genomics, National Cancer Center Research Institute, Tokyo, Japan
- 36 17. Laboratory of Molecular Medicine, Human Genome Center, The Institute of Medical Science,
37 The University of Tokyo, Tokyo, Japan
- 38 18. Department of Cancer Genome Informatics, Graduate School of Medicine/Faculty of
39 Medicine, Osaka University, Osaka, Japan
- 40 19. PRESTO, Japan Science and Technology Agency, Saitama, Japan

- 41 20. Graduate School of Public Health and Health Policy, City University of New York, New York,
42 USA.
43 21. Institute for Implementation Science in Population Health, City University of New York, New
44 York, USA.
45 22. Italian Institute for Genomic Medicine (IIGM), Turin, Italy.
46 23. Department of Molecular Biology of Cancer, Institute of Experimental Medicine, Prague,
47 Czech Republic.
48 24. Huntsman Cancer Institute and Department of Population Health Sciences, University of
49 Utah, Salt Lake City, Utah, USA
50 25. Division of Clinical Epidemiology and Aging Research, German Cancer Research Center
51 (DKFZ), Heidelberg, German
52 26. German Cancer Consortium (DKTK), German Cancer Research Center (DKFZ), Heidelberg,
53 German
54 27. Faculty of Healthy Sciences, University of Southern Denmark, Odense, Denmark
55 28. Max Delbrück Centre for Molecular Medicine, Berlin, Germany
56 29. Department of Bioinformatics, Biocenter, University of Würzburg, Würzburg, Germany

57
58 ‡. Present Address: Institute of Science and Technology for Brain-Inspired Intelligence, Fudan
59 University, Shanghai 200433, China
60

61 + These authors jointly supervised the work. Correspondence should be addressed to
62 zeller@embl.de, bork@embl.de or arumugam@sund.ku.dk

63 * These authors contributed equally to the work.
64
65
66

67 **ABSTRACT**

68

69 Association studies have linked microbiome alterations with many human diseases, but not always
70 reported consistent results, which necessitates cross-study comparisons. Here, a meta-analysis of
71 eight geographically and technically diverse fecal shotgun metagenomic studies of colorectal cancer
72 (CRC, N = 768), which was controlled for several confounders, identified a core set of 29 species
73 significantly enriched in CRC metagenomes (FDR < 1E-5). CRC signatures derived from single
74 studies maintained accuracy in other studies. By training on multiple studies we improved detection
75 accuracy and disease specificity for CRC. Functional analysis of CRC metagenomes revealed
76 enriched protein and mucin catabolism genes and depleted carbohydrate degradation genes.
77 Moreover we inferred elevated production of secondary bile acids from CRC metagenomes
78 suggesting a metabolic link between cancer-associated gut microbes and a fat- and meat-rich diet.
79 Through extensive validations, this meta-analysis firmly establishes globally generalizable, predictive
80 taxonomic and functional microbiome CRC signatures as a basis for future diagnostics.

81

82

83 **INTRODUCTION**

84

85 Studying microbial communities colonizing the human body in a culture-independent manner has been
86 enabled by metagenomic sequencing technologies [1]. These have yielded glimpses into the complex
87 yet incompletely understood interactions between the gut microbiome – the microbial ecosystem
88 residing primarily in the large intestine – and its host [2]. To explore microbiome-host interactions in a
89 disease context, metagenome-wide association studies (MWAS) have begun to map gut microbiome
90 alterations in diabetes, inflammatory bowel disease, colorectal cancer and many other conditions [3-
91 12]. However, due to the many biological factors possibly influencing gut microbiome composition in
92 addition to the condition studied, a current challenge for MWAS is confounding, which can cause false
93 associations [13, 14]. This issue is further aggravated by a lack of standards in metagenomic data
94 generation and processing, making it difficult to disentangle technical from biological effects [15].

95

96 Robustness of microbiome-disease associations can be assessed through comparisons across
97 multiple metagenomic case-control studies, i.e. meta-analyses. These aim at identifying associations
98 that are consistent across studies and thus less likely attributable to biological or technical
99 confounders. Most informative are meta-analyses of populations from diverse geographic and cultural
100 regions. Previous microbiome meta-analyses based on 16S rRNA gene amplicon data found stark
101 technical differences between studies and the reported taxonomic disease associations were either of
102 low effect size or not well resolved [16-18]. In contrast, shotgun metagenomics enables analyses with
103 higher taxonomic resolution and of gene functions to improve statistical power for fine-mapping
104 disease-associated strains and aid in the interpretation of host-microbial co-metabolism. Thus far
105 however, meta-analyses of shotgun metagenomic data have either reported on features of general
106 dysbiosis in comparisons across multiple diseases [19], or have left it unclear how well microbiome

107 signatures generalize across studies of the same disease when data are rigorously separated to avoid
108 over-optimistic evaluations of their prediction accuracy [20].

109

110 Here, we present a meta-analysis of a total of eight studies of CRC including fecal metagenomic data
111 from 386 cancer cases and 392 tumor-free controls. After consistent data reprocessing, we examined
112 an initial set of five studies for CRC-associated changes in the gut microbiome. Firstly, we investigated
113 potential confounders, followed by identifying (univariate) microbial species associations, and inferring
114 species co-occurrence patterns in CRC. Secondly, we trained multivariable classification models for
115 recognition of CRC status, from both taxonomic and functional microbiome profiles and tested how
116 accurately these models generalized to data from studies not used for training. Moreover, we
117 evaluated performance improvements achieved by pooling data across studies and the disease-
118 specificity of the resulting classification models. Thirdly, targeted investigation of virulence and toxicity
119 genes as candidate functional biomarkers for CRC revealed several of these to be enriched in CRC
120 metagenomes indicative of their prevalence and potential relevance in CRC patients. Three additional,
121 more recent studies were finally used to independently validate these taxonomic and functional CRC
122 signatures.

123

124 **RESULTS**

125

126 **Consistent processing of published and new data for meta-analysis of CRC metagenomes**

127 In this meta-analysis we included four published studies which used fecal shotgun metagenomics to
128 characterize CRC patients compared to healthy controls (referred to by the country codes FR, AT, CN,
129 and US, corresponding to the respective main study population; see **Table 1, Supplementary Table**
130 **S1**, and Methods for inclusion criteria). For an additional fifth study population, we generated new
131 fecal metagenomic data from samples collected in Germany (herein abbreviated as DE); a subset of
132 samples from this patient collective were published previously (**Table 1, Methods**, [8]). These five
133 studies were conducted on three continents and differed in sampling procedures, sample storage, and
134 DNA extraction protocols. Notably, the fecal specimen of the US study were freeze-dried and stored at
135 -80°C for more than 25 years before DNA extraction and sequencing [10]. In all studies, however,
136 samples were collected prior to treatment, thus excluding cancer therapy as a potential confounding
137 effect [14, 21]. Most samples were even taken before bowel preparation for colonoscopy, with some
138 exceptions in the DE, CN and US studies (**Supplementary Table S2**). To ensure consistency in
139 bioinformatic analyses, all raw sequencing data were (re-)processed using mOTUs2 for taxonomic
140 profiling [22] and MOCAT2 for functional profiling [23].

141

142 **Univariate meta-analysis of species associated with CRC**

143 The first aim of the meta-analysis was to determine gut microbial species that are enriched or depleted
144 in CRC metagenomes in a consistent manner across the five study populations. However, as these
145 studies differed from one another in many biological and technical aspects, we first quantified the
146 effect of study-associated heterogeneity on microbiome composition. We contrasted this with other
147 potential confounders ('patient age', 'BMI', 'sex', 'sampling after colonoscopy', and 'library size');

148 additionally, 'smoking status', 'type II diabetes comorbidity', and 'vegetarian diet' where available
149 **Extended Data 1, Supplementary Table S3**). This analysis revealed the factor 'study' to have a
150 predominant impact on species composition, which is supported by a recent comparison of DNA
151 extraction protocols, as these typically differ between studies [15]. An analysis of microbial alpha and
152 beta diversity showed study heterogeneity to also have a larger effect on overall microbiome
153 composition than CRC in our data (**Extended Data 2**).

154

155 For the identification of microbial taxa significantly differing in abundance in CRC, parametric effect
156 size measures are not well established, because microbiome data is characterized by non-Gaussian
157 distributions with extreme dispersion; we thus used a generalisation of the fold change (**Extended**
158 **Data 3**) and non-parametric significance testing. In this permutation test framework [24] (herein
159 referred to as blocked univariate Wilcoxon tests) differential abundance in CRC can be assessed
160 while accounting for 'study' as a nuisance effect that is treated as a blocking factor; additionally,
161 motivated by our confounder analysis, we also blocked for 'colonoscopy' in all analyses (Methods,
162 **Extended Data 1**). To rule out spurious associations due to the compositional nature of microbial
163 relative abundance data, we additionally compared the results of this test with a method [25]
164 employing log-ratio transformation (and found highly correlated results, **Supplementary Fig. 1,**
165 **Supplementary Table S4**).

166

167 At a meta-analysis false discovery rate (FDR) of 0.005, we identified 94 microbial species to be
168 differentially abundant in the CRC microbiome, out of 849 species consistently detected across
169 studies (**Supplementary Table S4**, Methods). Among these, we focused on a core set of the 29 most
170 significant markers (FDR < 1E-5, **Fig. 1a**) for further analysis. The latter included members of several
171 genera previously associated with CRC, such as *Fusobacterium*, *Porphyromonas*, *Parvimonas*,
172 *Peptostreptococcus*, *Gemella*, *Prevotella*, and *Solobacterium* (**Fig. 1b**, [8-11]), and 8 additional
173 species without genomic reference sequences (meta-mOTUs, Methods, [22]) mostly from the
174 *Porphyromonas* and *Dialister* genera and the Clostridiales order (see **Extended Data 4** and
175 **Supplementary Table S4** for genus-level associations). Collectively, these 29 core CRC-associated
176 species show a previously underappreciated diversity of 11 Clostridiales species to be enriched in
177 CRC (**Fig. 1b**). In contrast to the majority of species that are more strongly affected by study
178 heterogeneity than by CRC status, 26 out of the 29 CRC-associated species varied more by disease
179 status (**Fig. 1d**).

180

181 All of the core CRC-associated species were enriched in patients and were often undetectable in
182 metagenomes from non-neoplastic controls. While previous studies were contradictory in the reported
183 proportion of positive versus negative associations [8, 9, 17, 20], our meta-analysis results are more
184 easily reconciled with a model in which – potentially many – gut microbes contribute to or benefit from
185 tumorigenesis than with the opposing model in which a lack of protective microbes contributes to CRC
186 development (**Fig. 1b**). Although these core taxonomic CRC associations were highly significant and
187 consistent, individual studies showed marked discrepancies in the species identified as significant
188 (**Fig. 1a**). Retrospective examination of the precision and sensitivity with which individual studies

189 detected this core of CRC-associated species showed relatively low sensitivity for the US study
190 (consistent with the original report [10]) and low precision of the AT study due to associations that
191 were not replicated in other studies (**Supplementary Fig. 2**).

192

193 Analyzing patient metagenomes for co-occurrences among the core set of 29 species that are strongly
194 enriched in the CRC microbiome revealed four species clusters with distinct taxonomic composition
195 (**Fig. 2a, Extended Data 5, Methods**). Two of them showed strong taxonomic consistency: Cluster 1
196 exclusively comprised *Porphyromonas* spp., and cluster 4 only contained members of the Clostridiales
197 order. In contrast, the other two clusters were taxonomically more heterogeneous with cluster 3
198 grouping together the species with highest prevalence in CRC cases (all among the ten most highly
199 significant markers), consistent with a co-occurrence analysis of one of the data sets included here
200 [11]. Cluster 2 contained species with intermediate prevalence.

201

202 Investigating whether these four clusters were associated with different tumor characteristics, we
203 found the *Porphyromonas* cluster 1 to be significantly enriched in rectal tumors (**Fig. 2b**), consistent
204 with the presence of superoxide dismutase genes in *Porphyromonas* genomes possibly conferring
205 tolerance to a more aerobic milieu in the rectum (**Extended Data 5**). The Clostridiales cluster 4 was
206 significantly more prevalent in female CRC patients. All species clusters showed a slight tendency
207 towards late-stage CRC (i.e. AJCC stages III and IV), but this was only significant for cluster 3.
208 Associations with patient age and BMI were weaker and not significant (**Extended Data 5**). To rule out
209 secondary effects due to differences in patient composition among studies, all of these tests were
210 corrected for study effects (by blocking for 'study' and 'colonoscopy', see Methods). At the level of
211 individual species, significant stage-specific enrichments could not be detected suggesting CRC-
212 associated microbiome changes to be less dynamic during cancer progression than previously
213 postulated [26], although fecal material may be less suitable to address this question than tissue
214 samples.

215

216 **Metagenomic CRC classification models**

217 To establish metagenomic signatures for CRC detection across studies in face of geographic and
218 technical heterogeneity, we developed multivariable statistical modeling workflows with rigorous
219 external validation to avoid prevailing issues of overfitting and over-optimistic reports of model
220 accuracy [19]. As a precaution against over-optimistic evaluation, these workflows are independent of
221 the above-described differential abundance analysis. Instead, LASSO (Least Absolute Shrinkage and
222 Selection Operator) logistic regression classifiers were employed to select predictive microbial
223 features and eliminated uninformative ones (Methods).

224

225 In a first step, we used abundance profiles from five studies including the 849 most abundant microbial
226 species and assessed how well classifiers trained in cross validation (CV) on one study generalize in
227 evaluations on the other four studies (study-to-study transfer of classifiers) (**Fig. 3a**). Within-study
228 cross-validation performance, as quantified by the Area Under the Receiver Operating Characteristics
229 (AUROC) curve, ranged between 0.69 and 0.92 and was generally maintained in study-to-study

230 transfer (AUROC dropping by 0.07 ± 0.12 on average) with two notable exceptions. First, in line with
231 the univariate analysis of species associations, CRC detection accuracy on the US study was lower
232 than for the other studies, both in cross-validation and in study-to-study transfer. This could potentially
233 be explained by the US fecal specimen, unlike in the other studies, being freeze-archived for >25
234 years before metagenomic sequencing [10]. Second, classifiers trained on the AT study did not
235 generalize as well to the other studies, consistent with low study precision seen in univariate meta-
236 analysis (**Supplementary Fig. 2**). Given the microbial co-occurrence clusters described above, we
237 wondered whether species-species interactions would provide additional information relevant for CRC
238 recognition that is not contained in species abundance profiles. However, nonlinear classifiers able to
239 exploit such interactions did not yield significantly better accuracies (**Supplementary Fig. 3**, see also
240 [27]), suggesting that the linear model based on few biomarkers (on average 17 species account for
241 more than 80% of the classifier weight, **Extended Data 6**) is near optimal for CRC prediction.

242

243 We further assessed if including data from all but one study in model training improves prediction on
244 the remaining held-out study (leave-one-study-out validation, LOSO). LOSO performance of species-
245 level models ranged between 0.71 and 0.91, and when disregarding the US study as an outlier was
246 ≥ 0.83 (**Fig. 3b**). This corresponds to a LOSO accuracy increase of 0.076 ± 0.03 compared to study-to-
247 study transfer. These results suggest that one can expect a CRC detection accuracy ≥ 0.8 (AUROC)
248 for any new CRC study using similarly generated metagenomic data. We moreover verified that
249 metagenomic CRC classification models trained on species composition were not biased for clinical
250 subgroups. With the exception of slightly more sensitive detection of late stage CRC ($P = 0.03$, mostly
251 originating from the US study, **Extended Data 7**), we did not observe any classification bias by patient
252 age, sex, BMI, or localization. Together this suggests that these metagenomic classifiers are unlikely
253 to be strongly confounded by the clinical parameters recorded.

254

255 Several previous studies comparing microbiome changes across multiple diseases reported primarily
256 general dysbiotic alterations and highlighted the need to examine the disease specificity of
257 microbiome signatures [17, 19]. Therefore, we assessed false positive (FP) predictions of our
258 metagenomic CRC classifiers on fecal metagenomes of type 2 diabetes [4, 5], Parkinson's disease
259 [12], ulcerative colitis and Crohn's disease [6, 7] patients, reasoning that classifiers relying on
260 biomarkers for general dysbiosis would yield an excess of FPs on these cohorts. However, our LOSO
261 classification models calibrated to have a false-positive rate (FPR) of 0.1 on CRC datasets in fact
262 maintained similarly low FPRs on other disease datasets ranging from 0.09 to 0.13 (**Fig. 3c**).
263 Interestingly, disease specificity of LOSO models was significantly improved over that observed for
264 classifiers trained on a single study, indicating that inclusion of multiple studies in the training set of a
265 classifier can substantially improve its specificity for a given disease.

266

267

268 **Functional metagenomic signatures for CRC**

269 As shotgun metagenomics data, in contrast to 16S rRNA gene amplicon data, allow for a direct
270 analysis of the functional potential of the gut microbiome, we examined how predictive metabolic

271 pathways and orthologous gene families differing in abundance between CRC patients and controls
272 would be of CRC status. When applying the same classification workflow as above to eggNOG
273 orthologous gene family abundances [28], CRC detection accuracy was very similar to that observed
274 for taxonomic models (**Fig. 3de**). AUROC values ranged from 0.70 to 0.81 for study-to-study transfer
275 (per-study averages, **Fig. 3e**) and from 0.78 to 0.89 in LOSO validation with a pattern of generalization
276 across studies resembling that for taxonomic classifiers. The accuracy of functional signatures did not
277 strongly depend on eggNOG as an annotation source, but was similar when based on other
278 comprehensive functional databases, such as KEGG [29] (**Extended Data 8**). When using individual
279 gene abundances from metagenomic gene catalogues as a classifier input [30], we observed higher
280 within-study cross-validation AUROC values of ≥ 0.96 in all studies, but lower generalization to other
281 studies (AUROC between 0.60 and 0.79) (**Extended Data 8**).

282

283 To explore changes in metabolic capacity of gut microbiomes from CRC patients more broadly, we
284 quantified gut metabolic modules (defined in [31]) and subjected these to the same differential
285 abundance analysis developed for microbial species. Gut metabolic modules with significantly higher
286 abundance (FDR < 0.01, Wilcoxon test blocked for study and colonoscopy) in CRC metagenomes
287 predominantly belonged to pathways for the degradation of amino acids, mucins (glycoproteins) and
288 organic acids. This clear trend was accompanied by a depletion of genes from carbohydrate
289 degradation modules (**Fig. 4ab**). Differences in all four high-level categories were highly significant (P
290 < 1E-6 in all cases, blocked Wilcoxon tests) and consistent across studies (**Fig. 4b**). Overall these
291 results establish a clear shift from dietary carbohydrate utilization in a healthy gut microbiome to amino
292 acid degradation in CRC consistent with an earlier report based on a subset of the data [8].
293 Correlation analysis suggests that increased capacity for amino acid degradation is mostly contributed
294 by CRC-associated Clostridiales (cf. cluster 4 in Fig. 2, **Supplementary Fig. 4**). About one half of
295 these metagenomic pathway enrichments are also in agreement with independent metabolomics data
296 suggesting increased availability of amino acids in epithelial cells or feces of CRC patients
297 (**Supplementary Table S5**, [32-36]). While the observed pathway enrichments could potentially result
298 from many factors, including unmeasured ones [13], they are consistent with established dietary risk
299 factors for CRC, which include red and processed meat consumption [37] and low fiber intake [38].

300

301 The large metagenomic data set analyzed here allowed us to quantify the prevalence of gut microbial
302 virulence and toxicity mechanisms thought to play a role in colorectal carcinogenesis. Prominent
303 examples include the *Fusobacterium nucleatum* adhesion protein A (encoded by the *fadA* gene), the
304 *Bacteroides fragilis* enterotoxin (*bft* gene) and colibactin produced by some *Escherichia coli* strains
305 (*pks* genomic island) [39, 40]. Moreover, intestinal *Clostridium* spp. are known to contribute to the
306 conversion of primary to secondary bile acids using several metabolic pathways including 7 α -
307 dehydroxylation, encoded in the *bai* operon [41]. The products of this 7 α -dehydroxylation pathway,
308 deoxycholate and lithocholate, are known hepatotoxins associated with liver cancer [42] and
309 hypothesized to also promote CRC [43]. Although intensely studied at a mechanistic level, these
310 factors are not (well) represented in general databases that can be used for metagenome annotation
311 (**Supplementary Fig. 5**). Thus, we built a targeted metagenome annotation workflow based on

312 Hidden Markov Models to identify and quantify virulence factors and toxicity pathways of interest in
313 CRC. Additionally, we used co-abundance clustering to infer operon completeness for factors encoded
314 by multiple genes (Methods, **Extended Data 9, Supplementary Fig. 5**). While *fadA*, *bft*, the *pks* island
315 and the *bai* operon were clearly detectable in deeply sequenced fecal metagenomes, they varied
316 broadly with respect to abundance, significance and cross-study consistency of enrichment (**Fig. 4c**):
317 *fadA* and *pks* were significantly enriched in CRC metagenomes ($P = 5.3E-10$ and $4.1E-4$ respectively),
318 whereas no significant abundance difference could be detected for *bft* in fecal metagenomes, despite
319 reports on its enrichment in the mucosa of CRC patients [44], its carcinogenic effect in mouse models
320 [45], and synergistic action with *pks* [46]. Our quantification of the *bai* operon showed a highly
321 significant enrichment in CRC metagenomes ($P = 1.6E-9$) observed across all five studies (**Fig. 4d**) at
322 an average abundance that exceeded *fadA* and *pks* copy numbers (**Fig. 4c**). Metagenome analysis
323 indicated that at least four Clostridiales species (including the well characterized *C. scindens* and *C.*
324 *hylemonae* [47, 48]) have a (near) complete 7α -dehydroxylation pathway contributing to the observed
325 enrichment of *bai* operon copies (**Extended Data 9**). To validate this finding and further explore its
326 value towards diagnostic application, we developed a targeted quantification assay for the *baiF* gene
327 based on quantitative PCR (qPCR, see Methods). Quantification of *baiF* by qPCR using genomic DNA
328 from 47 fecal samples of the DE study population was found to be similar to, yet more sensitive than
329 by metagenomics (**Fig. 4e**). Gut microbial *baiF* copy numbers clearly distinguished CRC patients from
330 controls ($P = 0.001$) at an AUROC of 0.77, which in this subset of samples is surpassed by only a
331 single species marker for CRC (**Extended Data 9**). Although consistent with increased deoxycholate
332 metabolite levels reported for serum and stool samples of CRC patients [49], this finding does not
333 imply 7α -dehydroxylation pathway activity. We therefore quantified *baiF* expression using RNA
334 extracts from the same set of fecal samples, and found also transcript levels to be elevated in CRC
335 patients (**Fig. 4f**). The observed weak correlation of *baiF* expression with genomic abundance (**Fig. 4f**)
336 might be explained by dynamic transcriptional regulation [47] and *bai* expression in feces might not
337 accurately reflect the tumor microenvironment. Taken together, these data suggest gut microbial
338 metabolic markers to be meaningful and highly predictive of CRC status.

339

340 **Validation of CRC signatures in independent study populations**

341 Even though CRC classification accuracy for both species and functions were evaluated on
342 independent data, we nonetheless sought to confirm it using two additional study populations from
343 Italy (IT1 and IT2, combined $N = 61$ CRC, $N = 62$ CTR, [27], see Methods, Table 1) and one from
344 Japan (JP, $N = 40$ CRC, $N = 40$ CTR, see Methods, Table 1). The overlap of single species
345 associations detected in the IT2 study and those from the meta-analysis was found to vary within the
346 range seen for the other studies, whereas for IT1 and JP the overlap was slightly lower (cf. study
347 precision in **Supplementary Fig. 2, Extended Data 10**). Nonetheless, the AUROC of LOSO
348 classification models based on species ranged between 0.79 and 0.81 and that for the classifiers
349 based on eggNOG from 0.71 to 0.92 (**Fig. 5ab**). We also validated CRC enrichment of *fadA*, *pks* and
350 *bai* genes in these three study populations (**Fig. 5c**). Altogether these results highlight consistent
351 alterations in the gut microbiome of CRC patients across eight study populations from seven countries
352 in three continents.

353

354 DISCUSSION

355

356 Through extensive and statistically rigorous validation, in which data from studies used for training is
357 strictly separated from that for testing, our meta-analysis firmly establishes that gut microbial
358 signatures are highly predictive of CRC (see also [27]). In particular metagenomic classifiers trained
359 on species profiles from multiple studies maintained an AUROC of at least 0.8 in seven out of eight
360 data sets and achieved an accuracy similar to the fecal occult blood test, a standard non-invasive
361 clinical test for CRC (**Supplementary Fig. 6**, cf. [8]). These results thus suggest that polymicrobial
362 CRC classifiers are globally applicable and can overcome technical and geographical study
363 differences, which we found to generally impact observed microbiome composition more than the
364 disease itself (**Fig. 1c**, **Extended Data 1, 2**). The generalization accuracy of classifiers across studies
365 seen here is higher than that reported in 16S rRNA gene amplicon sequencing studies, which are
366 characterized by even larger heterogeneity across studies [16, 18] (**Supplementary Fig. 7**).

367

368 Previous microbiome meta-analyses suggested that the majority of gut microbial taxa differing in any
369 given case-control study reflect general dysbiosis rather than disease-specific alterations illustrating
370 the difficulty of establishing disease-specific microbiome signatures [17, 19]. Here, by combining data
371 across studies for training (LOSO), we were able to develop disease-specific signatures that
372 maintained false positive control on diabetes and IBD metagenomes at a very similar level as for CRC
373 (**Fig. 3c**) despite these diseases having shared effects on the gut microbiome [17, 50] and an
374 increased comorbidity risk [51].

375

376 Although for diagnostic purposes, unresolved causality between microbial and host processes during
377 CRC development are not a central concern, elucidating the underlying mechanisms would greatly
378 enhance our understanding of colorectal tumorigenesis. Towards this goal, we developed both broad
379 and targeted annotation workflows for functional metagenome analysis. First, we found functional
380 signatures based on the abundances of orthologous groups of microbial genes to yield accuracies as
381 high as taxonomic signatures (**Fig. 3**), which raises the hope for future improvements in metagenome
382 annotation to translate into microbiome signature refinements. Second, by investigating potentially
383 carcinogenic bacterial virulence and toxicity mechanisms taking a targeted metagenome annotation
384 approach, we confirmed highly significant enrichments of the colibactin-producing *pks* gene cluster
385 and the *Fusobacterium nucleatum* adhesin *FadA* in CRC metagenomes (**Fig. 4c**). Our results support
386 the clinical relevance of these factors adding to the experimental evidence for their carcinogenic
387 potential [46, 52-54]. We further examined the *bai* operon, encoding enzymes that produce secondary
388 bile acids via 7 α -dehydroxylation, as an example of toxic host-microbial co-metabolism (see [27] for
389 another intriguing example). While α -dehydroxylated bile acids are established liver carcinogens [42],
390 their contribution to CRC is less clear [43]. Here, we have, for the first time, shown *bai* to be highly
391 enriched in stool from CRC patients (**Fig. 4cd**) and confirmed this finding at both the genomic and the
392 transcriptomic level using qPCR (**Fig. 4ef**). As *bai* enrichment (and expression) is likely a
393 consequence of a diet rich in fat and meat [55], it is intriguing to explore whether *bai* could be used as

394 a surrogate microbiome marker for such difficult-to-measure dietary CRC risk factors. To further
395 unravel the molecular underpinning of these dietary CRC risk factors, molecular pathological
396 epidemiology studies that investigate the mucosal microbiome as part of the tumor microenvironment,
397 hold great potential [56, 57]. However, they will require more comprehensive diet questionnaires,
398 medical records, and molecular tumor characterizations than are available for the study populations
399 analyzed here. In this context, carcinogens possibly contained in the virome also warrant further
400 investigation [58, 59], but for this goal, metagenomic data needs to be generated with protocols
401 optimized for virus enrichment [60].

402

403 Taken together, our results and those by Thomas, Manghi et al. [27], strongly support the promise of
404 microbiome-based CRC diagnostics. Both taxonomic and metabolic gut microbial marker genes
405 established in these meta-analyses could form the basis of future diagnostic assays that are
406 sufficiently robust, sensitive, and cost-effective for clinical application. The targeted qPCR-based
407 quantification of the *baiF* gene is a first step in this direction. Our metagenomic analysis of this and
408 other virulence and toxicity markers bridge to existing mechanistic work in preclinical models and
409 could enable future work aiming to precisely determine the contribution of gut microbiota to CRC
410 development.

411

412

413 **Data and Code Availability**

414 The raw sequencing data for the samples in the DE study that had not been published before (see
415 Methods), are made available in the European Nucleotide Archive (ENA) under the study identifier
416 PRJEB27928. Metadata for these samples are available as **Supplementary Table S6**.

417 For the other studies included here, the raw sequencing data can be found under the following ENA
418 identifiers: PRJEB10878 for [11], PRJEB12449 for [10], ERP008729 for [9], and ERP005534 for [8].
419 The independent validation cohorts can be found in SRA under the identifier SRP136711 for [27] and
420 in the DDBJ database under the ID DRA006684.

421 Filtered taxonomic and functional profiles used as input for the statistical modeling pipeline are
422 available in **Supplementary Data 1**.

423 The code and all analysis results can be found under https://github.com/zellerlab/crc_meta.

424

425

426 **Acknowledgements**

427 We are thankful to members of the Zeller, Bork and Arumugam groups for inspiring discussions.
428 Additionally, we thank Yan Ping Yuan and the EMBL Information Technology Core Facility for support
429 with high-performance computing as well as the EMBL Genomics Core Facility for sequencing
430 support. We are also grateful for advice from Bern Klaus, EMBL Centre for Statistical Data Analysis.
431 We acknowledge funding from EMBL, DKFZ, the Huntsman Cancer Foundation, the Intramural
432 Research Program of the National Cancer Institute, ETH Zürich, and the following external sources:
433 the European Research Council (CancerBiome ERC-2010-AdG_20100317 to P.B., Microbios ERC-
434 AdG-669830 to P.B., Meta-PG ERC-2016-STG-716575 to N.S.), the Novo Nordisk Foundation (grant

435 NNF10CC1016515 to M.A.), the Danish Diabetes Academy supported by the Novo Nordisk
436 Foundation and TARGET research initiative (Danish Strategic Research Council [0603-00484B] to
437 M.A.), the Matthias-Lackas Foundation (to C.M.U), the National Cancer Institute (grants R01
438 CA189184, R01 CA207371, U01 CA206110, P30 CA042014 all to C.M.U), the BMBF (the de.NBI
439 network #031A537B to P.B. and the ERA-NET TRANSCAN project 01KT1503 to C.M.U.), the Helmut
440 Horten Foundation (to S.Sunagawa), and the Fundação de Amparo à Pesquisa do Estado de São
441 Paulo (FAPESP - 16/23527-2 to A.M.T.).

442 For the IT Validation Cohorts, funding was provided by Lega Italiana per La Lotta contro i Tumori.

443 For the JP Validation Cohort, funding was provided by the National Cancer Center Research and
444 Development Fund (25-A-4,28-A-4, and 29-A-6), Practical Research Project for Rare/Intractable
445 Diseases from the Japan Agency for Medical Research and Development (AMED) (JP18ek0109187),
446 JST (Japan Science and Technology Agency)-PRESTO (JPMJPR1507), JSPS (Japan Society for the
447 Promotion of Science) KAKENHI (16J10135, 142558 and 221S0002), Joint Research Project of the
448 Institute of Medical Science, the University of Tokyo, and the Takeda Science Foundation and
449 Suzuken Memorial Foundation.

450

451 **Competing Interest**

452 P. Bork, G. Zeller, A.Y. Voigt, and S. Sunagawa are named inventors on a patent (EP2955232A1:
453 Method for diagnosing colorectal cancer based on analyzing the gut microbiome).

454

455 **Author Contributions**

456 G.Z., M.A., P.B. conceived and supervised the study. P.S.-K., N.H., C.M.U., H.B., E.V., R.S. recruited
457 patients and collected samples. E.K., A.Y.V., S.Sunagawa, P.B. generated metagenomic data. A.M.,
458 P.T.P., J.S.F., A.P., S.Sunagawa, L.P.C., G.Z., M.A. developed metagenomic profiling workflows
459 and/or performed taxonomic and functional profiling. J.W., G.Z., K.Z., P.T.P., A.K., M.A., N.S.
460 performed statistical analysis and/or developed statistical analysis workflows. E.K. and R.P.P.
461 designed and performed validation experiments, A.M.T., P.M., S.G., D.S., S.M., H.S., S.Shiba, T.S.,
462 S.Y., T.Y., L.W., A.N., N.S. provided additional validation data, J.W., G.Z., M.A., P.T.P., P.B. designed
463 figures. G.Z., J.W., M.A., P.B., wrote the manuscript with contributions from P.T.P., A.M.,
464 S.Sunagawa, L.P.C., E.K., A.Y.V., E.V., R.S., P.S.K., H.B., E.N., N.S., L.W. All authors discussed and
465 approved the manuscript.

466

467

468 **Figure Captions**

469

470 **Figure 1. Despite study differences, meta-analysis identifies a core set of gut microbes**
471 **strongly associated with CRC.**

472 **(a)** Meta-analysis significance of gut microbial species derived from blocked Wilcoxon tests (n=574
473 independent observations) is given by bar height (false discovery rate, FDR, of 0.05). **(b)** Underneath,
474 species-level significance as computed by two-sided Wilcoxon test (FDR-corrected P-value) and
475 generalized fold change (Methods) within individual studies are displayed as heatmaps in gray and

476 color, respectively (see color bars and Table 1 for details on studies included). Species are ordered by
477 meta-analysis significance and direction of change. **(c)** For a core of highly significant species (meta-
478 analysis FDR 1E-5), association strength is quantified by the area under the Receiver Operating
479 Characteristics curve (AUROC) across individual studies (color coded diamonds) and 95% confidence
480 intervals are indicated by gray lines. Family-level taxonomic information is color-coded above species
481 names (numbers in brackets are mOTU species identifiers, see Methods). **(d)** Variance explained by
482 disease status (CRC vs controls) is plotted against variance explained by study effects for individual
483 microbial species with dot size proportional to abundance (Methods); core microbial markers are
484 highlighted in red. *F. nucleatum* – *Fusobacterium nucleatum*.

485

486 **Figure 2. Co-occurrence analysis of CRC-associated gut microbial species reveals four**
487 **clusters preferentially linked to specific patient subgroups.**

488 **(a)** The heatmap shows for all CRC patients (n=285 independent samples) if the respective sample is
489 positive for each of the core set of microbial marker species (see Methods for adjustment of positivity
490 threshold). Samples are ordered according to the sum of positive markers and marker species are
491 clustered based on Jaccard similarity of positive samples, resulting in four clusters (Methods). Barplots
492 in **(b)**, **(c)**, and **(d)** show the fraction of CRC samples that are positive for marker species clusters
493 (defined as the union of positive marker species) broken down by patient subgroups based on
494 differences in tumor location, sex, or CRC stage, respectively. Statistically significant associations
495 between CRC subgroups and marker species clusters were identified using the Cochran–Mantel–
496 Haenszel test blocked for study effects and are indicated above bars ($P < 0.1$).

497

498 **Figure 3. Both taxonomic and functional metagenomic classification models generalize across**
499 **studies in particular when trained on data from multiple studies.**

500 CRC classification accuracy resulting from cross validation within each study (gray boxes along
501 diagonal) and study-to-study model transfer (external validations off diagonal) as measured by
502 AUROC for classifiers trained on **(a)** species and **(d)** eggNOG gene family abundance profiles. The
503 last column depicts the average AUROC across external validations. Classification accuracy, as
504 evaluated by AUROC on a held-out study, improves if taxonomic **(b)** or functional **(e)** data from all
505 other studies are combined for training (leave-one-study-out, LOSO validation) relative to models
506 trained on data from a single study (study-to-study transfer, average and standard deviation shown).
507 Bar height for study-to-study transfer corresponds to the average of four classifiers (error bars indicate
508 standard deviation, n=4). **(c)** Combining training data across studies substantially improves CRC
509 specificity of the (LOSO) classification models relative to models trained on data from a single study
510 (depicted by bar color, as in (c) and (d)) as assessed by the false positive rate (FPR) on fecal samples
511 from patients with other conditions (see legend). Bar height for study-to-study transfer corresponds to
512 the average FPR across classifiers (n=5) with error bars indicating the standard deviation of FPR
513 values observed.

514

515 **Figure 4. Meta-analysis identifies consistent functional changes in CRC metagenomes.**

516 **(a)** Meta-analysis significance of gut metabolic modules derived from blocked Wilcoxon tests (n=574
517 independent samples) is indicated by bar height (top panel, FDR of 0.01). Underneath, the
518 generalized fold change (Methods) for gut metabolic modules [31] within individual studies is displayed
519 as heatmap (see color key below (b)). Metabolic modules are ordered by significance and direction of
520 change. A higher-level classification of the modules is color-coded below the heatmap for the four
521 most common categories (colors as in (b), white indicating other classes). **(b)** Normalized log
522 abundances for these selected functional categories is compared between controls (CTR) and
523 colorectal cancer cases (CRC). Abundances are summarized as geometric mean of all modules in the
524 respective category and statistical significance determined using blocked Wilcoxon tests (n=574
525 independent samples, see Methods). **(c)** Normalized log abundances for virulence factors and toxins
526 compared between metagenomes of controls (CTR) and colorectal cancer cases (CRC) (significant
527 differences $P < 0.05$ were determined by blocked Wilcoxon test, n=574 independent samples, see
528 Methods for gene identification and quantification in metagenomes; *fadA*: gene encoding
529 *Fusobacterium nucleatum* adhesion protein A, *bft*: gene encoding *Bacteroides fragilis* enterotoxin, *pks*:
530 genomic island in *Escherichia coli* encoding enzymes for the production of genotoxic colibactin, and
531 *bai*: bile acid inducible operon present in some Clostridiales species encoding bile acid converting
532 enzymes). **(d)** Meta-analysis significance (uncorrected P-value) as determined by blocked Wilcoxon
533 tests (n=574 independent samples) and generalized fold change within individual studies are
534 displayed as bars and heatmap, respectively, for the genes contained in the *bai* operon. Due to high
535 sequence similarity to *baiF*, *baiK* was not independently detectable with our approach. **(e)**
536 Metagenomic quantification of *baiF* (metag. ab. – normalized relative abundance) is plotted against
537 qPCR quantification in genomic DNA (gDNA) extracted from a subset of DE samples (n=47), with
538 Pearson correlation (r) indicated (see Methods). **(f)** Expression of *baiF* determined via qPCR on
539 reverse-transcribed RNA from the same samples in contrast to genomic DNA (as in e). The boxplots
540 on the side of (e), (f) show the difference between cancer (CRC) and control (CTR) samples in the
541 respective qPCR quantification (P-values on top were computed using a one-sided Wilcoxon test). All
542 boxplots show interquartile ranges (IQR) as boxes with the median as a black horizontal line and
543 whiskers extending up to the most extreme points within 1.5-fold IQR.

544

545 **Figure 5. Meta-analysis results are validated in three independent study populations**

546 CRC classification accuracy for independent datasets, two from Italy and one from Japan (see
547 **Supplementary Table S2**), is indicated by bar height for single study (white) and leave-one-study-out
548 (grey) models using either **(a)** species or **(b)** eggNOG gene family abundance profiles (cf. Fig. 3). Bar
549 height for single study models corresponds to the average of five classifiers (error bars indicate
550 standard deviation, n=5). **(c)** Normalized log abundances for virulence factors and toxins (cf. Figure
551 4c) compared between controls (CTR) and colorectal cancer cases (CRC). P-values were determined
552 by blocked, one-sided Wilcoxon tests (n=193 independent samples). Boxes represent interquartile
553 ranges (IQR) with the median as a black horizontal line and whiskers extending up to the most
554 extreme points within 1.5-fold IQR.

555

556

557 **Table 1. Fecal metagenomic studies of colorectal cancer included in this meta-analysis.**
 558 See Methods for inclusion criteria and **Supplementary Table S2** for extended meta-data. For a
 559 detailed description of patient recruitment and data generation for the DE study, see Methods. The
 560 data for 38 samples from the DE study had been published previously as part of an independent
 561 validation cohort in [8].

Country Code	Reference	No. of cases	No. of controls
FR	Zeller et al., 2014 [8]	53	61
AT	Feng et al., 2015 [9]	46	63
CN	Yu et al., 2017 [11]	74	54
US	Vogtmann et al., 2016 [10]	52	52
DE	this study	60	60
External validation cohorts			
IT1	[27]	29	24
IT2	[27]	32	28
JP	Courtesy of T. Yamada et al.	40	40

562
 563
 564

565 References

- 566 1. Tringe, S.G. and E.M. Rubin, *Metagenomics: DNA sequencing of environmental samples*.
 567 Nat. Rev. Genet., 2005. **6**(11): p. 805-814.
- 568 2. Tremaroli, V. and F. Bäckhed, *Functional interactions between the gut microbiota and host*
 569 *metabolism*. Nature, 2012. **489**(7415): p. 242-249.
- 570 3. Lynch, S.V. and O. Pedersen, *The Human Intestinal Microbiome in Health and Disease*. N.
 571 Engl. J. Med., 2016. **375**(24): p. 2369-2379.
- 572 4. Qin, J., et al., *A metagenome-wide association study of gut microbiota in type 2 diabetes*.
 573 Nature, 2012. **490**(7418): p. 55-60.
- 574 5. Karlsson, F.H., et al., *Gut metagenome in European women with normal, impaired and*
 575 *diabetic glucose control*. Nature, 2013. **498**(7452): p. 99-103.
- 576 6. Qin, J., et al., *A human gut microbial gene catalogue established by metagenomic*
 577 *sequencing*. Nature, 2010. **464**(7285): p. 59-65.
- 578 7. Schirmer, M., et al., *Dynamics of metatranscription in the inflammatory bowel disease gut*
 579 *microbiome*. Nat Microbiol, 2018. **3**(3): p. 337-346.
- 580 8. Zeller, G., et al., *Potential of fecal microbiota for early-stage detection of colorectal cancer*.
 581 Mol. Syst. Biol., 2014. **10**(11): p. 766.
- 582 9. Feng, Q., et al., *Gut microbiome development along the colorectal adenoma-carcinoma*
 583 *sequence*. Nat. Commun., 2015. **6**: p. 6528.
- 584 10. Vogtmann, E., et al., *Colorectal Cancer and the Human Gut Microbiome: Reproducibility with*
 585 *Whole-Genome Shotgun Sequencing*. PLoS One, 2016. **11**(5): p. e0155362.

- 586 11. Yu, J., et al., *Metagenomic analysis of faecal microbiome as a tool towards targeted non-*
587 *invasive biomarkers for colorectal cancer.* Gut, 2017. **66**(1): p. 70-78.
- 588 12. Bedarf, J.R., et al., *Functional implications of microbial and viral gut metagenome changes in*
589 *early stage L-DOPA-naïve Parkinson's disease patients.* Genome Med., 2017. **9**(1): p. 39.
- 590 13. Schmidt, T.S.B., J. Raes, and P. Bork, *The Human Gut Microbiome: From Association to*
591 *Modulation.* Cell, 2018. **172**(6): p. 1198-1215.
- 592 14. Forslund, K., et al., *Disentangling type 2 diabetes and metformin treatment signatures in the*
593 *human gut microbiota.* Nature, 2015. **528**(7581): p. 262-266.
- 594 15. Costea, P.I., et al., *Towards standards for human fecal sample processing in metagenomic*
595 *studies.* Nat. Biotechnol., 2017. **35**(11): p. 1069-1076.
- 596 16. Lozupone, C.A., et al., *Meta-analyses of studies of the human microbiota.* Genome Res.,
597 2013. **23**(10): p. 1704-1714.
- 598 17. Duvallet, C., et al., *Meta Analysis Of Microbiome Studies Identifies Shared And Disease-*
599 *Specific Patterns.* 2017.
- 600 18. Shah, M.S., et al., *Leveraging sequence-based faecal microbial community survey data to*
601 *identify a composite biomarker for colorectal cancer.* Gut, 2018. **67**(5): p. 882-891.
- 602 19. Pasoli, E., et al., *Machine Learning Meta-analysis of Large Metagenomic Datasets: Tools and*
603 *Biological Insights.* PLoS Comput. Biol., 2016. **12**(7): p. e1004977.
- 604 20. Dai, Z., et al., *Multi-cohort analysis of colorectal cancer metagenome identified altered*
605 *bacteria across populations and universal bacterial markers.* Microbiome, 2018. **6**(1): p. 70.
- 606 21. Maier, L., et al., *Extensive impact of non-antibiotic drugs on human gut bacteria.* Nature, 2018.
607 **555**(7698): p. 623-628.
- 608 22. Milanese, A., et al., *Microbial abundance, activity, and population genomic profiling with*
609 *mOTUs.* Nature Communications, 2019. **formally accepted for publication.**
- 610 23. Kultima, J.R., et al., *MOCAT2: a metagenomic assembly, annotation and profiling framework.*
611 *Bioinformatics*, 2016. **32**(16): p. 2520-2523.
- 612 24. Hothorn, T., et al., *A Lego System for Conditional Inference.* Am. Stat., 2006. **60**(3): p. 257-
613 263.
- 614 25. Mandal, S., et al., *Analysis of composition of microbiomes: a novel method for studying*
615 *microbial composition.* Microb Ecol Health Dis, 2015. **26**: p. 27663.
- 616 26. Tjalsma, H., et al., *A bacterial driver-passenger model for colorectal cancer: beyond the usual*
617 *suspects.* Nat Rev Microbiol, 2012. **10**(8): p. 575-82.
- 618 27. Thomas, A.M., et al., *Metagenomic analysis of colorectal cancer datasets identifies cross-*
619 *cohort microbial diagnostic signatures and a link with choline degradation.* co-submitted to
620 Nature Medicine, 2018.
- 621 28. Huerta-Cepas, J., et al., *eggNOG 4.5: a hierarchical orthology framework with improved*
622 *functional annotations for eukaryotic, prokaryotic and viral sequences.* Nucleic Acids Res.,
623 2016. **44**(D1): p. D286-93.
- 624 29. Kanehisa, M., et al., *Data, information, knowledge and principle: back to metabolism in KEGG.*
625 *Nucleic Acids Res.*, 2014. **42**(Database issue): p. D199-205.
- 626 30. Li, J., et al., *An integrated catalog of reference genes in the human gut microbiome.* Nat.
627 *Biotechnol.*, 2014. **32**(8): p. 834-841.
- 628 31. Vieira-Silva, S., et al., *Species-function relationships shape ecological properties of the human*
629 *gut microbiome.* Nat Microbiol, 2016. **1**(8): p. 16088.
- 630 32. Hirayama, A., et al., *Quantitative metabolome profiling of colon and stomach cancer*
631 *microenvironment by capillary electrophoresis time-of-flight mass spectrometry.* Cancer Res,
632 2009. **69**(11): p. 4918-25.
- 633 33. Denkert, C., et al., *Metabolite profiling of human colon carcinoma--deregulation of TCA cycle*
634 *and amino acid turnover.* Mol Cancer, 2008. **7**: p. 72.
- 635 34. Mal, M., et al., *Metabotyping of human colorectal cancer using two-dimensional gas*
636 *chromatography mass spectrometry.* Anal Bioanal Chem, 2012. **403**(2): p. 483-93.
- 637 35. Weir, T.L., et al., *Stool microbiome and metabolome differences between colorectal cancer*
638 *patients and healthy adults.* PLoS One, 2013. **8**(8): p. e70803.
- 639 36. Goedert, J.J., et al., *Fecal metabolomics: assay performance and association with colorectal*
640 *cancer.* Carcinogenesis, 2014. **35**(9): p. 2089-2096.
- 641 37. Aykan, N.F., *Red meat and colorectal cancer.* Oncology Reviews, 2015. **9**(1).
- 642 38. World Cancer Research Fund / American Institute for Cancer Research, *Diet, Nutrition,*
643 *Physical Activity and Cancer: a Global Perspective*, in *Continuous Update Project Expert*
644 *Report.* 2018.
- 645 39. Dutilh, B.E., et al., *Screening metatranscriptomes for toxin genes as functional drivers of*
646 *human colorectal cancer.* Best Pract Res Clin Gastroenterol, 2013. **27**(1): p. 85-99.

- 647 40. Sears, C.L. and W.S. Garrett, *Microbes, Microbiota, and Colon Cancer*. Cell Host Microbe, 2014. **15**(3): p. 317-328.
- 648
- 649 41. Ridlon, J.M., et al., *Consequences of bile salt biotransformations by intestinal bacteria*. Gut Microbes, 2016. **7**(1): p. 22-39.
- 650
- 651 42. Yoshimoto, S., et al., *Obesity-induced gut microbial metabolite promotes liver cancer through senescence secretome*. Nature, 2013. **499**(7456): p. 97-101.
- 652
- 653 43. Ajouz, H., D. Mukherji, and A. Shamseddine, *Secondary bile acids: an underrecognized cause of colon cancer*. World Journal of Surgical Oncology, 2014. **12**(1): p. 164.
- 654
- 655 44. Boleij, A., et al., *The Bacteroides fragilis toxin gene is prevalent in the colon mucosa of colorectal cancer patients*. Clin. Infect. Dis., 2015. **60**(2): p. 208-215.
- 656
- 657 45. Wu, S., et al., *A human colonic commensal promotes colon tumorigenesis via activation of T helper type 17 T cell responses*. Nat. Med., 2009. **15**(9): p. 1016-1022.
- 658
- 659 46. Dejea, C.M., et al., *Patients with familial adenomatous polyposis harbor colonic biofilms containing tumorigenic bacteria*. Science, 2018. **359**(6375): p. 592-597.
- 660
- 661 47. Ridlon, J.M., D.J. Kang, and P.B. Hylemon, *Isolation and characterization of a bile acid inducible 7alpha-dehydroxylating operon in Clostridium hylemonae TN271*. Anaerobe, 2010. **16**(2): p. 137-46.
- 662
- 663
- 664 48. Mallonee, D.H., W.B. White, and P.B. Hylemon, *Cloning and sequencing of a bile acid-inducible operon from Eubacterium sp. strain VPI 12708*. Journal of Bacteriology, 1990. **172**(12): p. 7011-7019.
- 665
- 666
- 667 49. Ocvirk, S. and S.J.D. O'Keefe, *Influence of Bile Acids on Colorectal Cancer Risk: Potential Mechanisms Mediated by Diet-Gut Microbiota Interactions*. Curr. Nutr. Rep., 2017. **6**(4): p. 315-322.
- 668
- 669
- 670 50. Gevers, D., et al., *The treatment-naive microbiome in new-onset Crohn's disease*. Cell Host Microbe, 2014. **15**(3): p. 382-392.
- 671
- 672 51. Viennot, S., et al., *Colon cancer in inflammatory bowel disease: recent trends, questions and answers*. Gastroenterol. Clin. Biol., 2009. **33 Suppl 3**: p. S190-201.
- 673
- 674 52. Rubinstein, M.R., et al., *Fusobacterium nucleatum Promotes Colorectal Carcinogenesis by Modulating E-Cadherin/ β -Catenin Signaling via its FadA Adhesin*. Cell Host Microbe, 2013. **14**(2): p. 195-206.
- 675
- 676
- 677 53. Kostic, A.D., et al., *Fusobacterium nucleatum potentiates intestinal tumorigenesis and modulates the tumor-immune microenvironment*. Cell Host Microbe, 2013. **14**(2): p. 207-215.
- 678
- 679 54. Arthur, J.C., et al., *Intestinal inflammation targets cancer-inducing activity of the microbiota*. Science, 2012. **338**(6103): p. 120-123.
- 680
- 681 55. Reddy, B.S., *Diet and excretion of bile acids*. Cancer Res, 1981. **41**(9 Pt 2): p. 3766-8.
- 682
- 683 56. Ogino, S., et al., *Integrative analysis of exogenous, endogenous, tumour and immune factors for precision medicine*. Gut, 2018. **67**(6): p. 1168-1180.
- 684
- 685 57. Ogino, S., et al., *Molecular pathological epidemiology of colorectal neoplasia: an emerging transdisciplinary and interdisciplinary field*. Gut, 2011. **60**(3): p. 397-411.
- 686
- 687 58. Hannigan, G.D., et al., *Diagnostic Potential and Interactive Dynamics of the Colorectal Cancer Virome*. MBio, 2018. **9**(6).
- 688
- 689 59. zur Hausen, H., *Red meat consumption and cancer: reasons to suspect involvement of bovine infectious factors in colorectal cancer*. Int J Cancer, 2012. **130**(11): p. 2475-83.
- 690
- 691 60. Shkoporov, A.N., et al., *Reproducible protocols for metagenomic analysis of human faecal phageomes*. Microbiome, 2018. **6**(1): p. 68.
- 692
- 693
- 694

695 **Methods**

696

697 **Study inclusion and data acquisition**

698 We used PubMed to search for studies that published fecal shotgun metagenomic data of human
699 colorectal cancer patients and healthy controls. The search term, all hits, and the justification for
700 exclusion or inclusion are available in **Supplementary Table S1**. Raw fastq files were downloaded for
701 the four included studies from the European Nucleotide Archive, using the following ENA identifiers:
702 PRJEB10878 for [11], PRJEB12449 for [10], ERP008729 for [9], and ERP005534 for [8].

703

704 **DE study recruitment and sequencing**

705 The German (DE) study population data consist of 60 fecal CRC metagenomes, 38 of which were
706 sequenced and published in [8] under ENA accession ERP005534. The fecal metagenomes from
707 additional 22 CRC patients recruited for the same ColoCare study (DKFZ, Heidelberg, [61, 62]) were
708 sequenced later as part of this work. All fecal samples were collected after colonoscopy. Sixty gender-
709 and age-matched participants of the PRÄVENT study run by the same clinical investigators were
710 included as healthy controls; as these were not subjected to colonoscopy, the presence of
711 undiagnosed colorectal carcinomas cannot be completely ruled out but is expected to be unlikely due
712 to low prevalence of preclinical CRC in the general population [63].

713 Written informed consent was obtained from all additional 22 CRC patients and 60 controls. The study
714 protocol was approved by the institutional review board (EMBL Bioethics Internal Advisory Board) and
715 the ethics committee of the Medical Faculty at the University of Heidelberg. The study is in agreement
716 with the WMA Declaration of Helsinki and the Department of Health and Human Services Belmont
717 Report.

718 Genomic DNA was extracted from the fecal samples (preserved in RNALater) and libraries were
719 prepared as previously described [8]. Whole-genome shotgun sequencing was performed by using
720 Illumina HiSeq 2000 / 2500 / 4000 (Illumina, San Diego, USA) platforms at the Genomics Core
721 Facility, European Molecular Biology Laboratory, Heidelberg.

722

723 **Independent validation cohorts**

724 During the revision of this manuscript, we included three independent study populations for external
725 validation. Two of them were recruited in Italy (IT1 and IT2) with informed consent from all participants
726 and ethical approval by the Ethics committee of Azienda Ospedaliera of Alessandria and that of the
727 European Institute of Oncology of Milan. Shotgun fecal metagenomic data was generated as
728 described in [27].

729 The third study population was recruited in Japan (JP) with informed consent and ethical approval of
730 the institutional review boards of the National Cancer Center Japan - Research Institute and the Tokyo
731 Institute of Technology. DNA was extracted from frozen fecal samples using a GNOME DNA Isolation
732 Kit (MP Biomedicals, Santa Ana, CA) with an additional bead-beating step as previously described
733 [64]. DNA quality was assessed with an Agilent 4200 TapeStation (Agilent Technologies, Santa Clara
734 CA). After final precipitation, the DNA samples were resuspended in TE buffer and stored at -80°C
735 before further analysis. Sequencing libraries were generated with the Nextera XT DNA Sample

736 Preparation Kit (Illumina, San Diego, CA). Library quality was confirmed with an Agilent 4200
737 TapeStation. Whole-genome shotgun sequencing was carried out on the HiSeq2500 platform
738 (Illumina). All samples were paired-end sequenced with a 150-bp read length to a targeted data set
739 size of 5.0 Gb.

740

741 **Taxonomic profiling and data preprocessing**

742 The metagenomic samples were quality controlled using MOCAT2's -rtf procedure, which is based on
743 the 'solexaqa' algorithm [23]. In particular, reads that map with at least 95% sequence identity and
744 alignment length of at least 45 bp to the human genome hg19 were removed. In a second step,
745 taxonomic profiles were generated with the mOTU profiler version 2.0.0 ([22, 65, 66] – see [motu-](http://motu-tool.org)
746 [tool.org](http://motu-tool.org) and GitHub version tag 2.0.0) using the following parameters: -l 75, -g 2 and -c. Briefly, this
747 profiler is based on ten universal single-copy marker-gene families (COG0012, COG0016, COG0018,
748 COG0172, COG0215, COG0495, COG0525, COG0533, COG0541 and COG0552) [66]. These
749 marker-genes were extracted from >25,000 reference genomes and >3,000 metagenomic samples
750 allowing to profile prokaryotic species with a sequenced reference genome (ref-mOTUs) and ones
751 without (meta-mOTUs). The read count for a mOTU was calculated as median of the read count of the
752 genes that belonged to that mOTU.

753 mOTU profiles were first converted to relative abundances to account for library size. Then, profiles
754 were filtered to focus on a set of species that are confidently detectable in multiple studies.
755 Specifically, microbial species that did not exceed a maximum relative abundance of 1E-03 in at least
756 3 of the studies were excluded from further analysis, together with the fraction of unmapped
757 metagenomic reads.

758

759 **Functional metagenome profiling and data preprocessing**

760 High-quality reads (same quality filtering as for taxonomic profiling) were aligned against a combined
761 database (IGChg38 hereafter) consisting of the hg38 release of the human reference genome and the
762 integrated gene catalog (IGC) containing 9.9 million non-redundant microbial genes [30] using BWA
763 mem [67] (Version: 0.7.15-r1140) with default parameters. The purpose of adding the human genome
764 to the reference database was to filter out reads that mapped as well or better to some human
765 sequence than to any bacterial gene. Alignments were computed separately for paired-end and single
766 read libraries (single reads could result from read pairs where one read was filtered out in the quality
767 filtering procedure described above). Alignments were then filtered to only retain those longer than
768 50bp with >95% sequence identity. Then the highest scoring alignment(s) was/were kept for each
769 read. As IGChg38 is a database of predominantly genes and not genomes, there will be a substantial
770 proportion of read-pairs where one end maps within the gene while the other end does not – it either
771 maps to an adjacent gene or remains unmapped due to intergenic regions not contained in the
772 database. Therefore, we counted a whole read-pair aligning to a gene when (i) both ends from a read
773 pair map to the same gene, (ii) only one end from a read-pair maps to the gene, or (iii) a read from the
774 single read library maps to the gene. We then counted only the read-pairs that map uniquely to one
775 gene in the IGC, thus excluding ambiguous read pairs mapping with similarly high scores to multiple
776 genes in the database. For a given metagenomic sample, we further normalized the abundance of

777 each IGC gene by the length of that gene. We then estimated relative abundance of IGC genes by
778 dividing gene abundances by the total abundance of all genes in IGC (excluding the human
779 chromosomes).

780 Because metagenomes from CRC patients were not included when the IGC was constructed, we
781 analyzed how well CRC-associated species as identified in this meta-analysis were represented in the
782 IGC. Using a phylogenetic marker gene (COG0533), which is also used by the species profiling
783 workflow on which the meta-analysis is based, for 24 out of the 29 core CRC-associated species we
784 found a match in the IGC with at least 90% nucleotide identity, indicating that a sequence from the
785 same species (above 93.1% identity) or a slightly more distant relative is present in the IGC
786 (**Supplementary Fig. 8**).

787 The relative abundance of eggNOG orthologous groups [28] was estimated by summing relative
788 abundances of genes annotated to belong to the same eggNOG orthologous group as of the most
789 recent annotations provided by MOCAT2 [23]. To obtain KEGG orthologous groups (KO) and pathway
790 abundances, we applied the same procedure, but using KEGG annotations for IGC provided by
791 MOCAT2 [29].

792

793 **Overview over statistical analyses**

794 For univariate association testing between the abundances of microbial taxa or gene functions we
795 used nonparametric tests throughout; all of these were two-sided Wilcoxon tests except were
796 otherwise noted. To account for potential confounding and heterogeneity between data sets we
797 employed a stratified version of the Wilcoxon test [24] (see below for details). ANOVA was conducted
798 on rank-transformed data. Significance of binary co-occurrence patterns was assessed using
799 (stratified) Cochran-Mantel-Haenszel tests.

800 Multivariable analysis was done with strict separation between training and test data. This importantly
801 also pertained to feature selection, which was either done via the LASSO [68] or by nested cross-
802 validation procedures to avoid overoptimistic performance assessment [69] (see below for details). All
803 samples included in this meta-analysis came from distinct individuals to ensure that generalization
804 across subjects – rather than across timepoints within a given subject – is assessed.

805

806 **Confounder analysis**

807 To quantify the effect of potential confounding factors relative to that of CRC on single microbial
808 species, we used an ANOVA-type analysis. The total variance within the abundance of a given
809 microbial species was compared to the variance explained by disease status and the variance
810 explained by the confounding factor akin to a linear model including both CRC status and confounding
811 factor as explanatory variables for species abundance. Variance calculations were performed on ranks
812 in order to account for non-Gaussian distribution of microbiome abundance data. Potential
813 confounders with continuous values were transformed into categorical data either as quartiles or for
814 the case of body mass index (BMI) into lean/obese/overweight according to conventional cutoffs (lean:
815 < 25, obese: 25 - 30, overweight: > 30).

816

817 **Univariate meta-analysis for the identification of CRC-associated gut microbial species**

818 Significance of differential abundance was tested on a per-species basis using a blocked Wilcoxon
819 test implemented in the R coin package [24]. Informed by the results of the preceding confounder
820 analysis, we blocked for `study` and additionally `colonoscopy` in the CN study. Within this framework,
821 significance is tested against a conditional null distribution derived from permutations of the observed
822 data. Notably, permutations are performed within each block in order to control for variations in block
823 size and composition. To adjust for multiple hypothesis testing, P-values were adjusted using the
824 false-discovery rate (FDR) method [70].

825 As nonparametric effect size measures we used the area under the ROC curve (AUROC) with
826 permutation-based confidence intervals computed using the pROC package in R [71]. We further
827 developed a generalization of the (logarithmic) fold change that is widely used for other types of read
828 abundance data. This generalization is designed to have better resolution for sparse microbiome
829 profiles (where 0 entries can render median-based fold change estimates uninformative for the large
830 portion of species with a prevalence below 0.5). The generalized fold change (gFC) is computed as
831 mean difference in a set of pre-defined quantiles of the logarithmic CTR and CRC distributions (see
832 **Extended Data 3** for further details; we used quantiles ranging from 0.1 to 0.9 in increments of 0.1).

833 For the retrospective analysis of study precision and recall for detecting microbial species associations
834 from the meta-analysis, the true set was defined as the species which were associated at a given FDR
835 in the meta-analysis. Then, we checked how well this set of species would be recovered using the
836 single-study significance as determined by the Wilcoxon test. Study precision corresponds to the
837 proportion of meta-analysis significant species among those detected as significant in a single study.
838 Similarly, recall (or sensitivity) corresponds to the proportion of species out of the true set of meta-
839 analysis significant species that were recovered in a given study.

840

841 **Species co-occurrence and cluster analysis in CRC metagenomes**

842 For the analysis of gut bacterial species co-occurring in CRC microbiomes, relative abundances of the
843 core set of associated species (excluding the CRC-depleted *Clostridiales* meta-mOTU [1296]) were
844 discretized into binary values to determine whether a CRC (metagenomic) sample is “positive” or
845 “negative” for a given microbial marker. To normalize for differences in prevalence (and therefore
846 specificity) of these markers we adjusted the threshold value, above which a sample is labeled
847 “positive” based on the abundance in healthy controls. For each microbial species, the 95th percentile
848 in healthy controls was used as threshold, which effectively results in adjusting the per-marker false
849 positive rate to 0.05. Based on the binarized species-by-sample matrix, species were then clustered
850 using the Jaccard dissimilarity as implemented in the vegan package in R [72]. Associations between
851 species clusters and meta-variables were tested as 2-by-n (where n is the number of categories in the
852 meta-variable tested) contingency tables using a Cochran-Mantel-Haenszel test with study as
853 blocking factor as implemented in the coin package [24].

854

855 **Multivariable statistical modeling workflow and model evaluation**

856 As a main goal of our work is to assess the generalization accuracy of microbiome-based CRC
857 classifiers across technical and geographic differences in patient populations, we extensively validated
858 classification models across studies taking the following two approaches.

859 In *study-to-study transfer* validation, metagenomic classifiers were trained on a single study and their
860 performance externally assessed on all other studies (off-diagonal cells in **Fig. 3ac**). Effectively we
861 implemented a nested cross validation procedure on the training study to compute within-study
862 accuracy (cells on the diagonal in **Fig. 3ac**) and tune the model hyperparameters.

863 In *leave-one-study-out* (LOSO) validation, data from one study was set aside as an external validation
864 set, while the data from the remaining 4 studies was pooled as a training set on which we
865 implemented the same nested cross validation procedure as for study-to-study transfer (see [19] for a
866 more detailed description of LOSO).

867 Data preprocessing, model building, and model evaluation was performed using the SIAMCAT R
868 package (<https://bioconductor.org/packages/SIAMCAT>, version **1.1.0**).

869

870 **Preprocessing of taxonomic abundance profiles for statistical modeling**

871 Relative abundances were first filtered to remove markers with low overall abundance and no variance
872 (an artifact for single-study data arising from the joint data filtering described above), log-transformed
873 (after adding a pseudo-count of 1E-05 to avoid non-finite values resulting from log(0), [73]) and finally
874 standardized as z-scores. Data were split into training and test set for 10 times repeated 10-fold
875 stratified cross validation (balancing class proportions across folds). For each split, a L1-regularized
876 (LASSO) logistic regression model [68] was trained on the training set, which was then used to predict
877 the test set. The lambda parameter, i.e. regularization strength was selected for each model to
878 maximize the area under the precision recall curve under the constraint that the model contained at
879 least 5 non-zero coefficients. Models were then evaluated by calculating the area under the Receiver
880 Operating Characteristics curve (AUROC) based on the posterior probability for the CRC class.

881 In model transfer to a hold-out study, the holdout data were normalized for comparability in the same
882 way as the training dataset by using the frozen normalization function in SIAMCAT, which retains the
883 same features and re-uses the same normalization parameters (e.g. the mean of a feature for z-score
884 standardization). Then, all 100 models derived from the cross validation on the training dataset (10
885 times repeated 10-fold CV) were applied to the holdout dataset and predictions were averaged across
886 all models.

887 In the LOSO setting, data from the four training studies were jointly processed as a single dataset in
888 the same way as described above using 10 times repeated 10-fold stratified cross validation.

889

890 **Preprocessing of functional abundance profiles**

891 Functional profiles, such as eggNOG gene family or KEGG module abundance profiles were
892 preprocessed as described above for species profiles, but using 1E-06 as maximum abundance cutoff
893 and 1E-09 as a pseudo-count during log transformation. Since these abundance tables contained
894 several thousand input features we implemented an additional feature selection step, which was
895 nested properly into the cross-validation procedures as described above. This nested approach is
896 crucial to avoid over-optimistically biased performance estimates ([74], Chapter 7.10). Specifically,
897 features were filtered inside each training fold (without using any information from the test fold) by
898 selecting the 1600 features with highest single-feature AUROC values (for features depleted in CRC,
899 1 - AUROC was used for feature selection).

900

901 **Preprocessing of gene abundance profiles**

902 To ascertain the predictive power of a classifiers based on IGC gene abundances [30] we applied a
903 series of filters to the abundance tables to reduce the number of genes that would be the input of the
904 LASSO modelling. These filters were applied once on a per-study level and once in a leave-one-
905 study-out (LOSO) mode, where they were applied jointly to all studies in the training set, with the
906 remaining one being held out for external validation.

907 The following filters were applied in this order:

- 908 1. All genes with 0 abundance in $\geq 15\%$ of samples (regardless of CRC status) were discarded.
- 909 2. The remaining data was discretized using the equal frequencies method implemented in the
910 'discretize' function of the sideChannelAttack R package (version 1.0-6) as a preparation to
911 the minimal-redundancy-maximal-relevance (mRMR) algorithm [75].
- 912 3. As a feature selection procedure, mRMR (code version from 20 April 2009 downloaded from
913 <http://home.penglab.com/proj/mRMR/> on 3 Dec 2016) was run on the gene abundance table
914 to retain the 100 top genes as output.

915 LASSO models were then built on log₁₀-transformed abundances (pseudo-count of 10E-09, centered
916 and scaled) of the sets of 100 top genes returned by mRMR. The whole process was repeated 10
917 times in a 5-fold stratified cross-validation scheme to allow for an estimation of the confidence of the
918 AUROCs of the resulting models. We used the Liblinear package (version 2.10-8) to build the LASSO
919 models in R and tested a sequence of 20 cost parameters (equivalent to the lambda parameter
920 controlling regularization strength) evenly spaced from 0.001^2 to 0.2^2 . The cost parameter was
921 selected to maximize the AUROC within the training set.

922

923 **External evaluation of disease-specificity of the metagenomic classifiers**

924 To assess how disease-specific the predictions of the CRC models are, we applied these to data from
925 case-control studies investigating other human diseases. Fecal metagenomic data of patients with
926 Parkinson's disease [12], type 2 diabetes [4, 5], and inflammatory bowel disease [6, 7] were
927 taxonomically profiled as described above. The parameters for quality control with MOCAT2 and for
928 the mOTU profiler were the same as described above, except for the data from [6], where we used -l
929 50 (to set the threshold for minimum alignment length to 50) as the read length is shorter (average
930 read length 71) compared to the other more recently generated Illumina shotgun metagenomic data.

931 Relative abundance data were treated exactly as another holdout dataset for each model, i.e. applying
932 the frozen normalization prediction routines as described above. For each CRC model applied to the
933 external datasets, a cutoff on its prediction output was adjusted to yield a false positive rate (FPR) of
934 0.1 on the controls of its respective (CRC) training set. Subsequently its FPR on metagenomes from
935 patients suffering from the above-mentioned (non-CRC) conditions was assessed to evaluate its
936 disease specificity. The rationale behind this is that a metagenomic classifier recognizing general
937 features of dysbiosis would be expected to predict CRC patients and those suffering from other
938 conditions at a similar rate; such a classifier would thus in the above-described evaluation display a
939 much higher FPR than on the controls of its training set. In contrast maintaining a low FPR in this

940 evaluation indicates that the classification model is based on CRC-specific features rather than
941 hallmarks of general dysbiosis or nonspecific inflammation.

942

943 **Functional profiling of gut metabolic modules (GMMs)**

944 Gut metabolic modules were computed as originally proposed [31], using the KEGG KO profiles based
945 on the IGC (see **Functional metagenome profiling** above) as input. Statistical analysis and
946 generalized fold change calculations were performed analogously to species profiles (see above). Gut
947 metabolic modules were summarized across functional groups (e.g. amino acid degradation) as
948 geometric mean of all modules within the respective group.

949

950 **Targeted functional analysis of virulence and toxicity pathways of potential relevance in CRC**

951 To investigate toxins and virulence mechanisms that have previously been implicated with CRC [40],
952 we constructed for each gene belonging to the respective virulence or toxicity pathway a hidden
953 Markov model (HMM). Each HMM was built from a multiple sequence alignment generated by
954 MUSCLE [76], containing the respective reference sequences and close homologs identified using
955 PSI-Blast [77]. Multiple sequence alignments are available together with the code for this paper
956 (https://github.com/zellerlab/crc_meta). Then, we screened the IGC metagenomic gene catalogue [30]
957 with each HMM using the HMMER software (version 3.1b2) [78]. Genes with an E-value below 1E-10
958 were filtered for uniqueness, since in some cases the HMMs would call different regions in the same
959 gene. For single gene virulence factors (i.e. *fadA* and *bft*), potential IGC hits were aligned against the
960 reference sequence using the Needleman-Wunsch algorithm in the EMBOSS package [79]. Hits were
961 then filtered based on percentage of sequence identity (cutoff: 40%) and sequence similarity to the
962 species relative abundance profiles based on maximum relative abundance (cutoff: 1E-07) in order to
963 exclude genes with limited relevance. Statistical analysis was performed on the sum of all genes.

964 For virulence pathways containing more than one gene, the IGC hits of each functional group within
965 the pathway were aligned against the respective reference sequence and filtered for percentage of
966 sequence identity and maximum abundance. Then, all hits were clustered based on the Pearson
967 correlation of the log-abundances across all samples using the Ward algorithm as implemented in the
968 *hclust* function in R. The gene clusters were filtered based on operon completeness (how many genes
969 of the operon were present in the cluster) and average correlation within the cluster (**Extended Data**
970 **9**). For statistical analysis, the genes in the selected gene clusters were summed up within each group
971 or all together for the overall analysis.

972

973 **Quantitative PCR for *baiF***

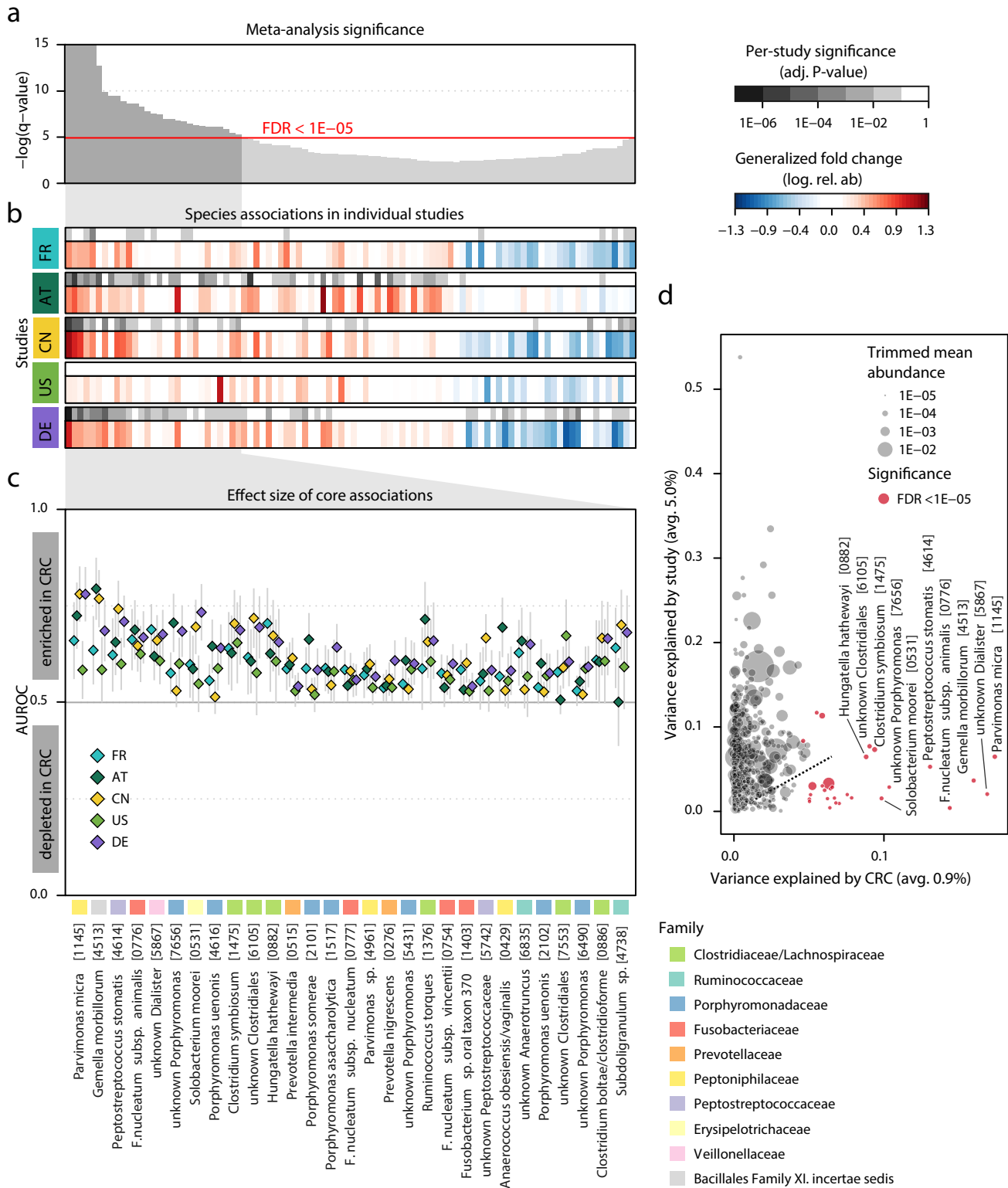
974 Real-time quantitative PCR to quantify the abundance and expression of *baiF* was performed on a
975 subset of samples in the DE cohort (20 control and 24 colorectal cancer samples, see
976 **Supplementary Table S6**). For these samples, DNA and RNA extraction was done with the Allprep
977 PowerFecal DNA/RNA kit (Qiagen, Cat No: 80244) with additional RNase and DNase digestion steps,
978 respectively, as described by the manufacturer. DNA and RNA concentrations were determined by
979 Qubit Fluorometer (Invitrogen) and quality control of all RNA samples was done using an Agilent 2100
980 Bioanalyzer in combination with RNA 6000 Nano and Pico LabChip kits.

981 First-strand cDNA was synthesized by SuperScript IV VILO Master Mix with ezDNase enzyme and
 982 random hexamer primers (Invitrogen, catalogue number 11766500) as recommended by the
 983 manufacturer. Reaction were performed as described in the protocol with one minor change of
 984 temperature (incubation for the reverse transcription step at 55°C).
 985 To quantify *baiF* relative to the total bacterial RNA/DNA in a sample, qPCR was performed in
 986 triplicates for 16S rRNA and the *baiF* genes, using both cDNA and genomic DNA (gDNA) as template.
 987 We used the following primers for *baiF*: TTCAGYTTCTACACCTG (forward),
 988 GGTTTRCCATRCCGAACAGCG (reverse), and standard primers F515 and R806 for 16S [80]. RT-
 989 PCR reactions were prepared with a final primer concentration of 0.5 μ M, including 5 ng of genomic
 990 DNA or 10 ng of cDNA in 20 μ l final reaction volume, and reactions were performed with SYBR Green
 991 qPCR mix on StepOne Real-Time PCR system (Thermo Fisler Scientific). Cycling conditions were as
 992 follows; initial denaturation of 95°C for 10 min, then 40 cycles of denaturing at 95°C for 15 s, annealing
 993 at 60°C for 60 s followed by melt curve analysis.
 994 Delta-Ct values were calculated as difference between *baiF* and 16S Ct values. Significance of the
 995 comparison between control and colorectal cancer samples was tested on the delta-Ct values using a
 996 one-sided Wilcoxon test as a confirmation of metagenomic enrichment.
 997

998 Additional References

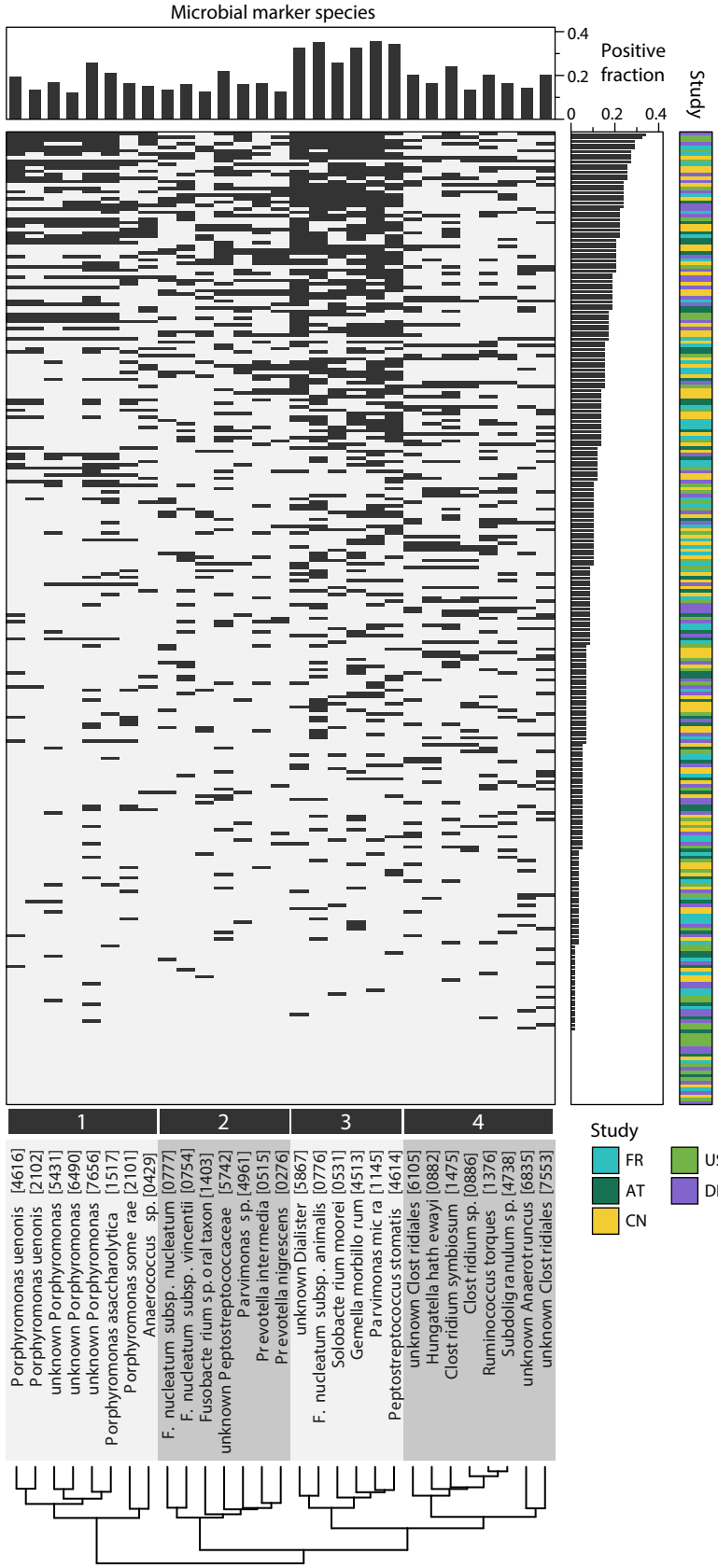
- 999 61. Bohm, J., et al., *Discovery of novel plasma proteins as biomarkers for the development of*
 1000 *incisional hernias after midline incision in patients with colorectal cancer: The ColoCare study.*
 1001 *Surgery*, 2017. **161**(3): p. 808-817.
 1002 62. Liesenfeld, D.B., et al., *Metabolomics and transcriptomics identify pathway differences*
 1003 *between visceral and subcutaneous adipose tissue in colorectal cancer patients: the ColoCare*
 1004 *study.* *Am J Clin Nutr*, 2015. **102**(2): p. 433-43.
 1005 63. Pox, C.P., et al., *Efficacy of a nationwide screening colonoscopy program for colorectal*
 1006 *cancer.* *Gastroenterology*, 2012. **142**(7): p. 1460-7 e2.
 1007 64. Furet, J.P., et al., *Comparative assessment of human and farm animal faecal microbiota using*
 1008 *real-time quantitative PCR.* *FEMS Microbiol Ecol*, 2009. **68**(3): p. 351-62.
 1009 65. Mende, D.R., et al., *Accurate and universal delineation of prokaryotic species.* *Nat. Methods*,
 1010 2013. **10**(9): p. 881-884.
 1011 66. Sunagawa, S., et al., *Metagenomic species profiling using universal phylogenetic marker*
 1012 *genes.* *Nat. Methods*, 2013. **10**(12): p. 1196-1199.
 1013 67. Li, H. and R. Durbin, *Fast and accurate short read alignment with Burrows-Wheeler transform.*
 1014 *Bioinformatics*, 2009. **25**(14): p. 1754-60.
 1015 68. Tibshirani, R., *Regression Shrinkage and Selection via the Lasso.* *J.R. Stat. Soc. Series B*
 1016 *Stat. Methodol.*, 1996. **58**(1): p. 267-288.
 1017 69. Smialowski, P., D. Frishman, and S. Kramer, *Pitfalls of supervised feature selection.*
 1018 *Bioinformatics*, 2010. **26**(3): p. 440-3.
 1019 70. Benjamini, Y. and Y. Hochberg, *Controlling the false discovery rate: a practical and powerful*
 1020 *approach to multiple testing.* *J. R. Stat. Soc. Series B Stat. Methodol.*, 1995. **57**(1): p. 289–
 1021 300.
 1022 71. Robin, X., et al., *pROC: an open-source package for R and S+ to analyze and compare ROC*
 1023 *curves.* *BMC Bioinformatics*, 2011. **12**(1).
 1024 72. Oksanen, J., et al., *vegan: Community Ecology Package.* 2018.
 1025 73. Costea, P.I., et al., *A fair comparison.* *Nat. Methods*, 2014. **11**(4): p. 359-359.
 1026 74. Hastie, T., R. Tibshirani, and J. Friedman, *The Elements of Statistical Learning: Data Mining,*
 1027 *Inference, and Prediction.* 2013: Springer Science & Business Media. 536.
 1028 75. Peng, H., F. Long, and C. Ding, *Feature selection based on mutual information: criteria of*
 1029 *max-dependency, max-relevance, and min-redundancy.* *IEEE Trans Pattern Anal Mach Intell*,
 1030 2005. **27**(8): p. 1226-38.

- 1031 76. Edgar, R.C., *MUSCLE: multiple sequence alignment with high accuracy and high throughput*.
1032 Nucleic Acids Res., 2004. **32**(5): p. 1792-1797.
- 1033 77. Altschul, S.F., et al., *Gapped BLAST and PSI-BLAST: a new generation of protein database*
1034 *search programs*. Nucleic Acids Res., 1997. **25**(17): p. 3389-3402.
- 1035 78. Eddy, S.R., *Accelerated Profile HMM Searches*. PLoS Comput. Biol., 2011. **7**(10): p.
1036 e1002195.
- 1037 79. Rice, P., I. Longden, and A. Bleasby, *EMBOSS: the European Molecular Biology Open*
1038 *Software Suite*. Trends Genet., 2000. **16**(6): p. 276-277.
- 1039 80. Caporaso, J.G., et al., *Global patterns of 16S rRNA diversity at a depth of millions of*
1040 *sequences per sample*. Proc Natl Acad Sci U S A, 2011. **108 Suppl 1**: p. 4516-22.
- 1041

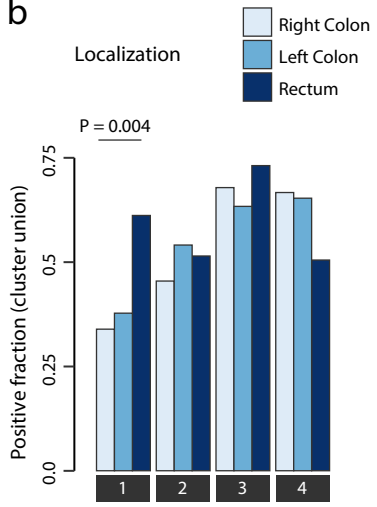


a

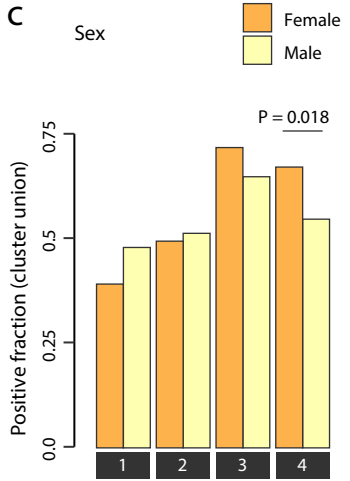
Colorectal cancer metagenomes (Sample positive for this marker species)



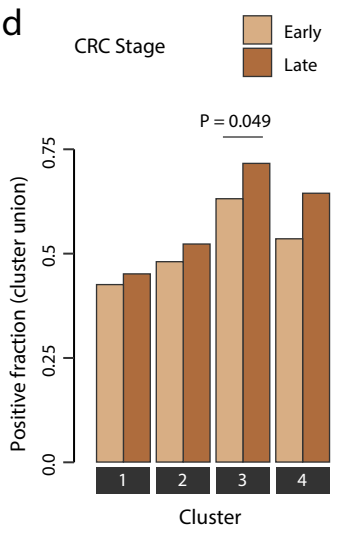
b



c

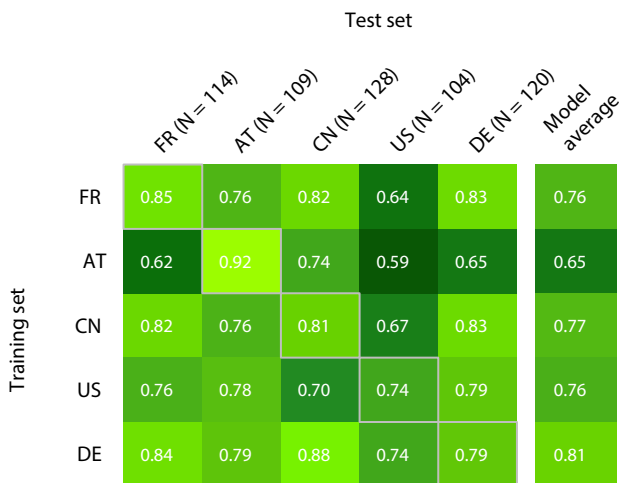


d



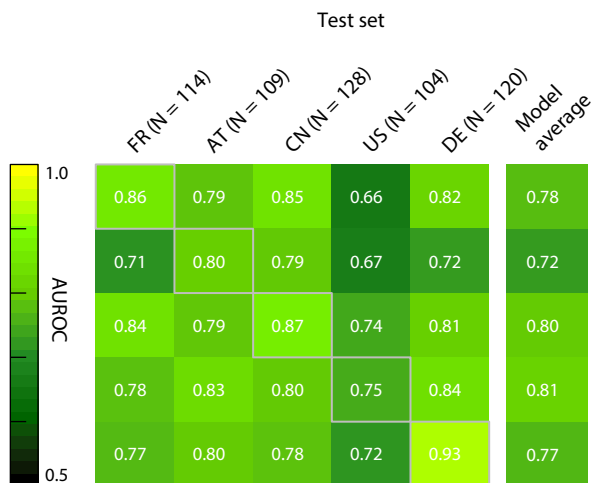
a

Classification models based on species

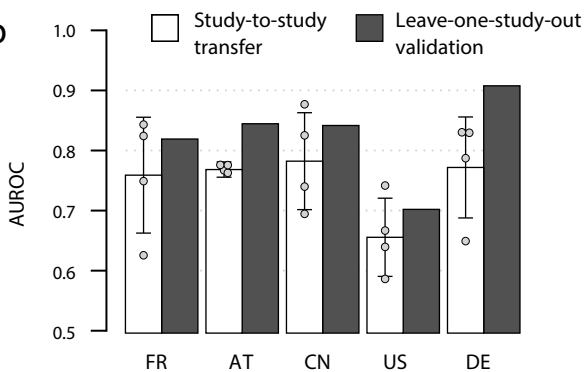


d

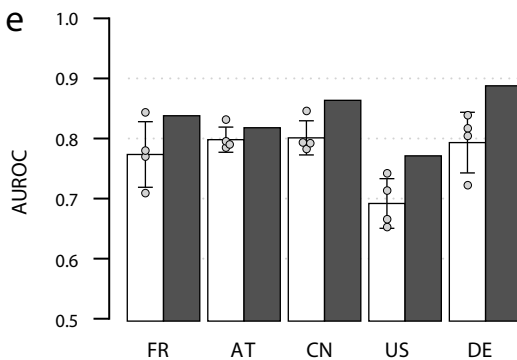
Classification models based on eggNOG



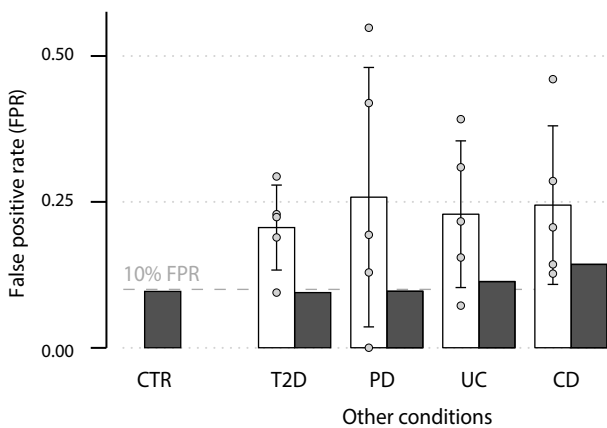
b



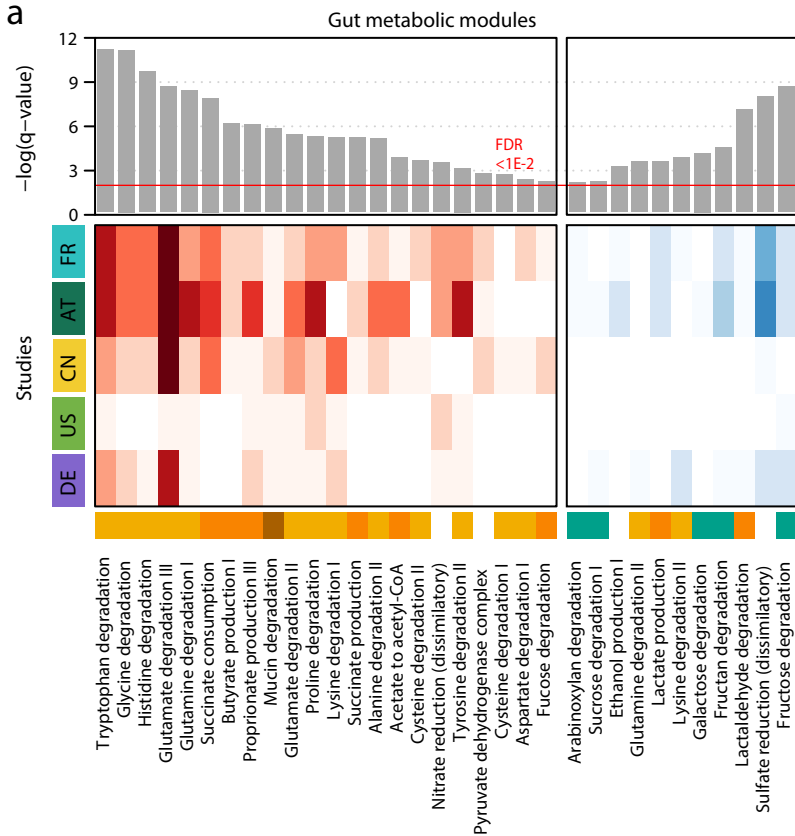
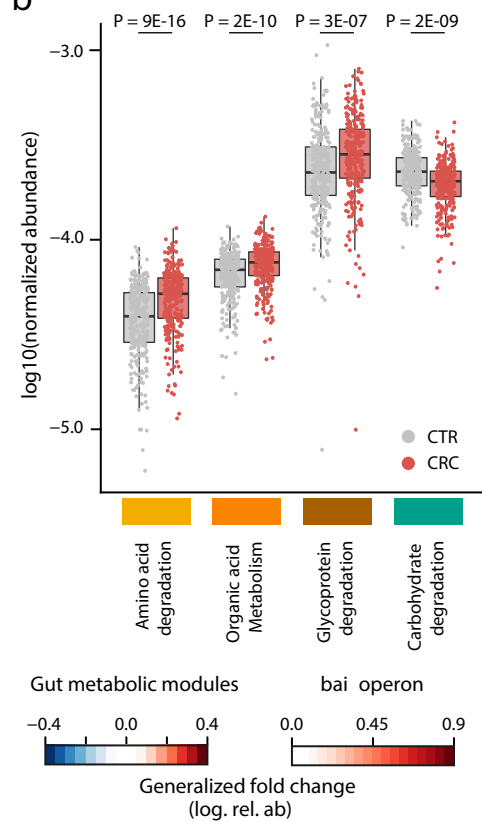
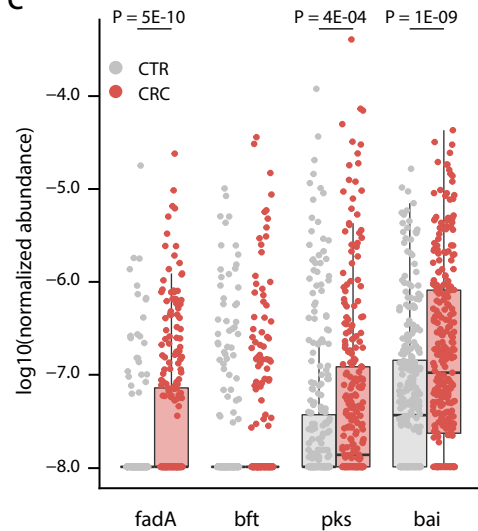
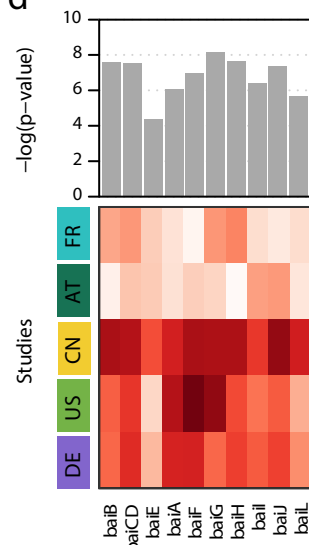
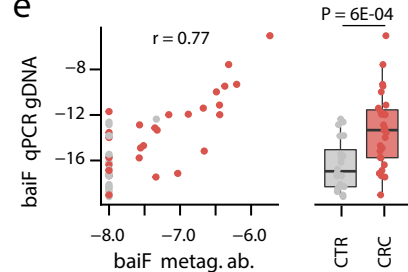
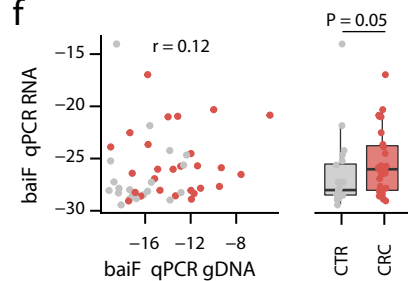
e

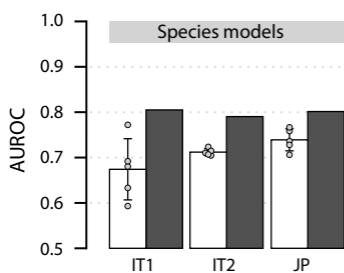
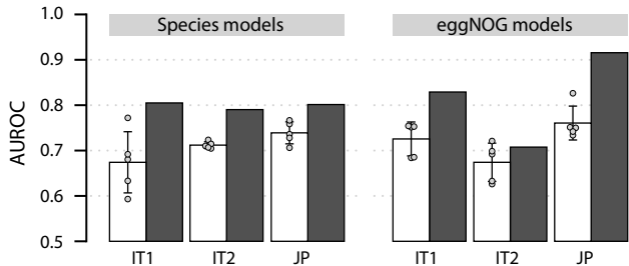


c



Abbr.	Condition	N
CTR	Healthy controls from meta-analysis	290
T2D	Type 2 diabetes	201
PD	Parkinson 's disease	31
UC	Ulcerative colitis	98
CD	Crohn 's disease	63

a**b****c****d****e****f**

a**b****c**